



ASSESSMENT OF GEOMETRIC CHANGES IN REGION OF INTEREST AND ITS DOSIMETRIC CONSEQUENCES USING DEFORMABLE IMAGE REGISTRATION FOR HEAD AND NECK ADAPTIVE RADIATION THERAPY

Sümeýra CAN¹, Didem KARAÇETİN²

¹⁻²Istanbul Basakşehir Cam and Sakura City Hospital

*sumeyracn@gmail.com,

BAŞ VE BOYUN ADAPTİF RADYOTERAPİ İÇİN DEFORMABLE GÖRÜNTÜ KAYDI KULLANILARAK İLGİLİ BÖLGEDEKİ GEOMETRİK DEĞİŞİMLERİN VE DOZİMETRİK SONUÇLARIN DEĞERLENDİRİLMESİ

ABSTRACT:

The aim of this study was to evaluate the change in volume and center of mass for a region of interest (ROI) and how changes affect the cumulative dose through Geometric Processing Unit (GPU)-based Deformable Image Registration. Ten head and neck cancer patients treated with simultaneous integrated boost in tomotherapy were analyzed retrospectively. Planning computed tomography (CT) and pretreatment weekly CT images were obtained for each patient. Cumulative dose and geometric changes were calculated for critical organs using these images, GPU-based image recording. The cumulative dose was evaluated according to geometric changes and compared with the planned dose. There was no statistical difference between the cumulative dose and the planned dose for D_{mean}, V_{100%} and V_{90%} of planning target volume (PTV₁) ($p > 0.05$). However, the cumulative dose was 14.8% and 8.8% lower than the planned dose for V_{100%} and V_{95%} of PTV₃, respectively. The cumulative dose delivered to the spinal cord was 7% higher than the planned dose; however, 6.6% and 4.1% were less than the planned dose for the left and right parotid glands, respectively. Because head and neck cancer patients undergo many anatomical changes during treatment, cumulative dose assessment is an important parameter for determining how well treatment planning is actually being achieved. GPU-based three dimensional (3D) deformable image registration enables real-time assessment of dose accumulation and tracking of inter-fraction volume variation for a region of interest. Deformable image recording is an important tool for the evaluation of adaptive radiotherapy.

Key Words : Adaptive Radiotherapy, Deformable Image Registration, Head and Neck Cancers, Radiation Dose, Tomotherapy

ÖZET:

Bu çalışmanın amacı, ilgilenilen bir bölge için hacim ve kütle merkezindeki değişimi ve değişikliklerin kümülatif dozu nasıl etkilediğini Geometrik İşlem Birimi (GPU) tabanlı deforme edilebilir görüntü kaydı yoluyla değerlendirmektir. Tomoterapide simültane entegre boost ile tedavi edilen on baş boyun kanseri hastası retrospektif olarak analiz edildi. Her hasta için planlama BT ve tedavi öncesi elde edilen haftalık BT görüntüleri elde edildi. Bu görüntüler, GPU tabanlı görüntü kaydı kullanılarak kritik organlar için kümülatif doz ve geometrik değişiklikler hesaplandı. Kümülatif doz geometrik değişikliklere göre değerlendirildi ve planlanan doz ile karşılaştırıldı. Planlanan hedef hacmin (PTV₁) D_{mean}, V₁₀₀ ve V₉₀'i için kümülatif doz ile planlanan doz arasında istatistiksel bir fark yoktu ($p > 0.05$). Ancak kümülatif doz, PTV₃'ün V₁₀₀ ve V₉₅'i için sırasıyla planlanan dozdan sırasıyla %14,8 ve %8,8 oranında daha düşük olduğu görüldü. Medulla spinalise verilen kümülatif doz, planlanan dozdan %7 daha yüksekti; ancak sol ve sağ parotid bezleri için sırasıyla planlanan dozdan sırasıyla %6,6 ve %4,1 daha azdı. Baş boyun kanseri hastaları tedavi boyunca birçok anatomik değişiklik geçirdiğinden kümülatif doz değerlendirmesi tedavi planlamasının ne kadar gerçekte sağlandığını belirlemek için önemli bir parametredir. GPU tabanlı 3 boyutlu (3D) deforme edilebilir görüntü kaydı, gerçek zamanlı doz birikiminin değerlendirilmesini ve ilgilenilen bir bölge için fraksiyonlar arası hacim değişiminin takip edilmesini sağlar. Deforme edilebilir görüntü kaydı, adaptif radyoterapinin değerlendirilmesi için önemli bir araçtır.

Anahtar Kelimeler: Adaptif radyoterapi, Baş boyun kanserleri, Deforme edilebilir görüntü kaydı, Radyasyon dozu, Tomoterapi

*Corresponding author: Sumeýra CAN, PhD, ¹⁻²Istanbul Basakşehir Cam and Sakura City Hospital Istanbul Basakşehir Cam and Sakura City Hospital, Başakşehir Mah. G-434 Cad. No: 2L Başakşehir / İSTANBULTÜRKİYE, mail: sumeyracn@gmail.com, Phone: +90 (553) 686 7040 ORCID:0000-0003-1991-9774

1. Introduction

Radiotherapy, along with surgery and/or chemotherapy, is the main treatment for head and neck cancers (Atwell, 2020). Modern therapy techniques, namely intensity modulated radiation therapy and volumetric arc radiation therapy, allow the delivery of the treatment dose to target volumes while simultaneously sparing critical structures. On the other hand, patients with head and neck cancer undergo many anatomical changes caused by weight loss during radiotherapy (Toledano, 2012). In addition, tumor volume and parotid gland volume decrease, and this decrease is usually asymmetrical (O'Daniel, 2007; Sharma, 2020;). Innovations in patient immobilization and imaging technology allow us to minimize setup uncertainties; however, there may be differences between planned and absorbed doses due to anatomical changes. Anatomical change can be evaluated using kilo-voltage computed tomography (kVCT) or mega voltage computed tomography (MVCT) scans with an advanced imaging system (Heukelom, 2020; Lowther, 2020; Kanehira, 2020).

Adaptive radiation therapy (ART) is to revise the original treatment plan based on the patient's random or systematic anatomical changes during 6-7 weeks of fractionated radiotherapy, thereby improving the quality of treatment (Capelle, 2012). In ART, the patient's CT image is taken again and after the new contouring and re-planning, the patient continues the treatment according to the new treatment plan. However, manual target critical structures delineation in offline ART takes time (Loo, 2011; Veiga, 2014). Recent studies have shown that deformable image registration (DIR) plays a crucial role in ART to monitor anatomical changes (Fung, 2020). In addition, it is possible to determine target volumes and calculate the cumulatively absorbed dose in the respective volumes via DIR, however, image quality is very important (Veiga, 2015; Zhang, 2018; Scaggion, 2020). Although MVCT scans can confirm the patient's position and anatomical change, they have lower quality than kVCT scans for soft tissues (Nobnop, 2019).

On the same ground, in this study, it was aimed to evaluate changes in volume and center of mass and how these changes affect the cumulative dose for the region of interest, considering patient-specific anatomy with Geometric Processing Unit (GPU)-based Deformable Image Registration.

2. Materials and Methods

2.1. Patient population and Target delineation

Ten head and neck cancer patients treated with Tomotherapy Hi-Art (Accuray Inc., Sunnyvale, CA, USA) using the simultaneous integrated boost (SIB) technique were selected for this study. Seven patients were diagnosed with tonsil malignant neoplasm, 1 patient with nasopharyngeal CA, and 2 patients with tonsil carcinoma. Weight changes in patients were recorded before and after treatment. Patient information is shown in Table 1.

Table 1. Patients' characteristic regarding treatment

Patient ID	Diagnosis	Prescription Dose (Gy)	Tx Duration (Day)	Weight Change (kg)
1	Tonsil CA	70.00	53	8.80
2	Base of Tongue	70.00	51	2.00
3	Nasopharynx	69.96	47	5.40
4	Tonsil CA	70.00	56	10.90
5	Tonsil CA	70.00	39	7.00
6	Tonsil CA	70.00	50	2.10
7	Tonsil CA	70.00	43	9.60
8	Tonsil CA	70.00	45	11.50
9	Tonsil CA	70.00	43	4.40
10	Base of Tongue	70.20	50	10.70

For treatment planning, a planning CT image with a slice thickness of 3 mm was taken for each patient. Three different target volumes were defined for each patient. Thermoplastic masks with head and neck micro-perforations were used for patient immobilization. All targets, including clinical target volume (CTV₁) (gross volume of disease), CTV₂ (next stage nodal regions), and CTV₃ (areas harboring subclinical disease) were contoured in relation to other anatomical boundaries of the structures. Tighter margins have been added to create planning target volumes (PTVs). Based on our clinical protocol, PTVs were generated from respective CTVs by adding a 3mm margin with all expansions for setup uncertainties. In addition to the parotid glands, brain stem, medulla spinalis, mandible, and oral cavity, optic nerves, lenses, and eyes were contoured for dosimetric analysis.

2.1. Treatment Planning and Evaluation

Helical tomotherapy plans were created with Accuray's integrated treatment planning system (TPS) Hi-Art PlanningStation 5.1.1.6 using the TomoTherapy (Accuray Inc., Sunnyvale, CA, USA) platform. The prescription dose of PTV₁ was 70 Gy in 35 fractions with a minimum coverage of 95% for all treatment plans while protecting as much critical structures as possible. In addition, 62.7 and 56.1 Gy were prescribed for PTV₂ and PTV₃, respectively. The field width was defined as 2.5 cm, the eigen factor was 0.277, and the modulation factor was 2.5. Dose restrictions for helical tomotherapy plans were optimized according to the Radiation Therapy Oncology Group (RTOG) 0615 protocol. Data from dose volume histograms (DVHs) of all plans were used to determine the dosimetric difference between the planned dose and the cumulative dose. V_{100%}, V_{95%}, V_{90%} (volume that receives 100%, 95%, 90% of prescription dose) and D_{mean} (mean dose) of target volumes were considered to evaluate tumor coverage. In addition, the maximum dose (D_{max}) for the spinal cord and brain stems was limited to <45 Gy and <54 Gy, respectively. Also, D_{mean} for the parotid glands was limited to <26 Gy. Also, D_{max} for lenses, optic nerves, eyes was taken into account.

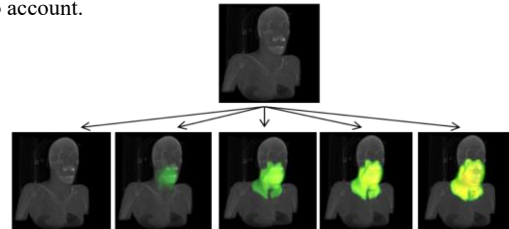


Figure 1. Tumor coverage and weekly delivered dose through DIR during 6 weeks of the treatment course for selected case. (Patient-3)

2.2. The change in volume and center of mass for ROI

Six to eight Daily kVCTs obtained to correct set-up errors before the treatment were selected for each patient in this study. In order to perform kV-to-kV registration, alignment was done to provide a close overlaid for two scans as much as possible, so, these kVCTs were superimposed on the planned CT images to delineate targets and critical structures. And then resizing and resampling of CT images were performed to track anatomical changes via GPU based deformable image registration algorithm. Deformation vector fields obtained based on each Cartesian direction were used for contour propagation to map the delineated ROI on planning CT to each weekly kVCT. A Jacobian analysis was performed for the deformed anatomy. In order to determine non-rigid change in the patient setup, deformation based on each contoured structure was evaluated. U, V, and W matrices were used for the Jacobian determinant for each voxel to evaluate the volumetric changes in the target volumes and surrounding critical structures. The determinant was defined as follows:

$$J_i = \begin{vmatrix} \frac{dU}{dx_i} & \frac{dU}{dy_i} & \frac{dU}{dz_i} \\ \frac{dV}{dx_i} & \frac{dV}{dy_i} & \frac{dV}{dz_i} \\ \frac{dW}{dx_i} & \frac{dW}{dy_i} & \frac{dW}{dz_i} \end{vmatrix} \quad (1)$$

The change in the center of mass and the distance between the PTVs and the left and right parotid glands were determined based on Cartesian coordinates using DIR helped to compensate for the inter-fractional motion of the target volumes and critical organs. The doses were then recalculated from each kVCT to determine the actual delivered dose to the targets and the critical structures. Linear interpolation was used for the dose mapping. The cumulative dose was calculated by summing, week by week, to obtain the total absorbed dose. In order to make a comparison between the accumulated dose and the planned dose, Gamma analysis was performed. Based on our model, all patients were treated identically, and the change in anatomy was not considered for dose distribution. For Gamma analysis, 1% and 1 mm were chosen as the default criteria. Gamma analysis was defined by:

$$\Gamma(\vec{r}_e, \vec{r}_r) = \sqrt{\frac{r^2(\vec{r}_e, \vec{r}_r)}{\Delta d^2} + \frac{\delta^2(\vec{r}_e, \vec{r}_r)}{\Delta D^2}} \quad (2)$$

where Δd and ΔD are the distance to agreement and HU difference criteria, respectively, r_e is the position at the evaluated pixel, and r_r is the position of the reference voxel (Guerrero, 2006).

2.3. Statistical analysis

Finally, SPSS statistical software version 28.0.1. (SPSS, Chicago, IL, USA) was used to examine the statistical differences in each of the planned dose obtained from helical tomotherapy plans and the delivered dose obtained by a GPU-based 3D image deformation/visualization tool. A paired sampled t-test was applied to determine the difference between planned and accumulated doses. For this study, according to the null hypothesis, there should be no difference between the mean planned dose and the mean cumulative dose. In addition, correlation analysis was applied to evaluate the effect of geometric changes in volume and center of mass (COM) displacement on the delivered dose to both parotid glands. Based on Pearson's correlation, it was measured whether there is a linear dependence between the aforementioned variables. Pearson's correlation was defined by:

$$r = \frac{\sum(x - m_x)(y - m_y)}{\sqrt{\sum(x - m_x)^2} \sqrt{\sum(y - m_y)^2}} \quad (3)$$

where m_x and m_y were the mean of geometric changes in volume and COM displacement, respectively. The p value (significance level) of the correlation was calculated based on the t value, which is defined by:

$$t = \frac{r}{\sqrt{1-r^2}} \sqrt{n-2} \quad (4)$$

Statistical significance of $p < 0.05$ was considered for both analyses. If the p value was $< 5\%$, the correlation was considered statistically significant.

3. Results

3.1. Cumulative dose for PTVs

Based on the Jacobian and Gamma analysis, the accumulated dose versus planned dose was evaluated for ROI. Planned and accumulated doses for target volumes were listed in Table 2 and Table 3, respectively. According to the test results, there was no statistical difference between the accumulated dose and the planned dose for D_{mean} , $V_{100\%}$ and $V_{90\%}$ of PTV₁ ($p > 0.05$); however, there was a statistical difference between the planned dose and the accumulated dose for $V_{95\%}$ of PTV₁ with a maximum difference of 8.6%. The accumulated dose was $\sim 3\%$ lower than the planned dose for $V_{95\%}$ of PTV₁; however, the planned dose was delivered to PTV₁ as expected considering D_{mean} , $V_{100\%}$ and $V_{90\%}$. Tumor coverage and weekly delivered dose for the selective case was shown in Figure 1. Additionally, there was no statistical difference between the accumulated dose and the planned dose for PTV₂ ($p > 0.05$); however, dose differences were observed in $V_{100\%}$ and $V_{95\%}$ of PTV₃ ($p < 0.05$). The accumulated dose was 14.8% and 8.88% lower than the planned dose for $V_{100\%}$ and $V_{95\%}$ of PTV₃, respectively. The dosimetric comparison between planned and accumulated doses for target volumes was shown in Figure 2. All p-values and plan evaluations for the ROI were listed in Table 5. Moreover, weekly doses were shown in Figure 3 for target volumes from ten patients. As a result, the planned dose was delivered to the target volumes; however, dose discrepancies were observed for several parameters of PTVs in the patient where maximum weight loss was observed.

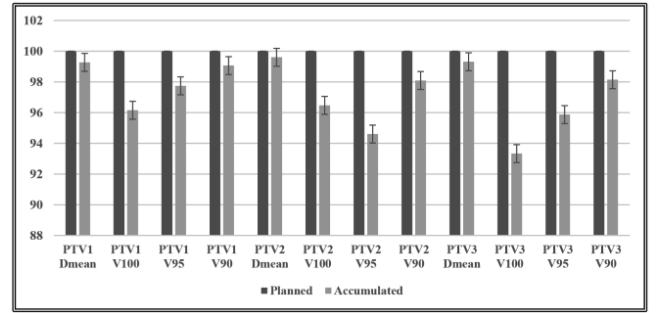


Figure 2. Dosimetric comparison between planned and accumulated dose for target volumes. All parameters are normalized to 100%

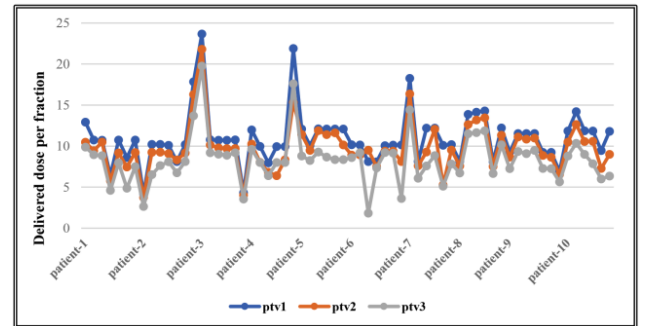


Figure 3. Weekly delivered dose were shown for target volumes from ten patients. $D_{95\%}$ of target volumes were considered.

Table 2: Planned dose of target volumes.

Patient ID	Planned Dose											
	PTV1				PTV2				PTV3			
	D _{mean}	V100	V95	V90	D _{mean}	V100	V95	V90	D _{mean}	V100	V95	V90
	Gy	(70 Gy)	(66.5 Gy)	(63 Gy)	Gy	(63 Gy)	(59.8 Gy)	(56.7 Gy)	Gy	(57 Gy)	(54.1 Gy)	(51.3 Gy)
1	70.97	91.40	99.85	100.00	71.21	94.03	100.00	100.00	70.46	78.62	92.46	96.54
2	70.75	87.63	97.66	99.77	70.80	86.88	99.90	100.00	66.90	94.09	99.34	95.32
3	71.00	86.57	96.59	98.35	64.54	99.53	99.79	99.92	66.87	89.87	98.62	97.94
4	71.72	91.17	99.70	99.97	68.93	91.17	99.70	93.57	57.56	94.94	99.94	100.00
5	70.94	90.03	98.93	99.69	68.74	90.03	98.93	98.01	57.40	99.91	99.97	100.00
6	70.96	92.31	99.44	99.79	67.52	96.89	92.31	90.88	64.47	94.29	94.32	96.89
7	71.10	88.28	99.42	99.99	70.66	94.29	98.14	99.98	66.91	88.28	94.17	99.56
8	70.81	80.01	95.18	98.75	67.23	96.13	99.40	96.60	58.25	91.99	98.00	99.62
9	67.01	86.57	98.23	99.39	65.56	91.99	98.98	90.60	58.48	92.22	96.28	99.23
10	71.01	91.34	99.82	100.00	66.11	93.28	99.56	99.91	61.93	93.42	94.09	99.24
Mean	70.14	88.53	98.48	99.57	68.13	93.42	98.67	96.94	62.92	91.76	96.71	98.43

Table 3: Accumulated dose of target volumes

Patient ID	Accumulated Dose											
	PTV1				PTV2				PTV3			
	D _{mean}	V100	V95	V90	D _{mean}	V100	V95	V90	D _{mean}	V100	V95	V90
	Gy	(70 Gy)	(66.5 Gy)	(63 Gy)	Gy	(63 Gy)	(59.8 Gy)	(56.7 Gy)	Gy	(57 Gy)	(54.1 Gy)	(51.3 Gy)
1	70.83	87.44	99.33	99.96	71.03	91.55	99.24	99.93	70.52	73.81	94.38	98.19
2	70.50	90.37	98.03	99.40	70.98	93.20	99.85	100.00	67.28	90.37	91.40	94.40
3	70.95	83.29	96.69	99.45	64.76	95.76	96.59	98.35	65.93	87.09	91.55	97.66
4	71.63	90.77	98.11	99.35	69.51	91.28	94.80	94.80	57.90	86.57	96.95	98.35
5	70.92	89.81	98.82	99.58	69.09	93.11	91.17	98.54	57.53	89.78	94.94	99.70
6	70.95	90.88	98.39	99.38	67.43	96.08	96.86	92.31	64.33	88.50	89.53	90.85
7	71.03	86.03	98.41	99.87	70.53	87.66	93.40	98.05	67.19	87.99	90.03	92.67
8	68.16	87.63	91.55	96.13	65.83	87.54	91.10	95.18	56.89	82.89	96.78	99.73
9	66.18	75.92	90.38	95.04	64.48	92.37	95.44	83.25	58.02	88.21	95.32	96.84
10	70.00	69.11	92.92	98.22	64.98	92.75	96.57	90.60	59.31	81.30	86.41	97.65
Mean	70.11	85.12	96.26	98.63	67.86	90.13	93.35	95.10	62.49	85.65	92.72	96.60

3.2. Cumulative dose for OARs

A paired sample t-test was also applied for the medulla spinalis and parotid glands. Overdose of the medulla spinalis was observed in two patients, and the accumulated dose was higher than the planned dose by 18.4% and 26.2% in Patient-7 and Patient-10, respectively. On the other hand, there was no statistical difference between the accumulated dose and planned dose considering all patient data for the medulla spinalis ($p = 0.211$). Additionally, there was a statistical difference between the planned dose and accumulated dose for the left parotid gland ($p = 0.045$), and the delivered dose was less than the planned dose by 6.6%. On the other hand, there was no statistical difference between the planned dose and accumulated dose for the right parotid gland ($p = 0.07$). Moreover, the accumulated dose was lower than the planned dose by ~ 4% for the right parotid gland. The weekly delivered doses of the left and right parotid glands from each patient were shown in Figure 4 and Figure 5. As a result, the planned dose was delivered to the organs at risk (OARs). The difference between the planned dose and the accumulated dose for critical structures was given in Table 4.

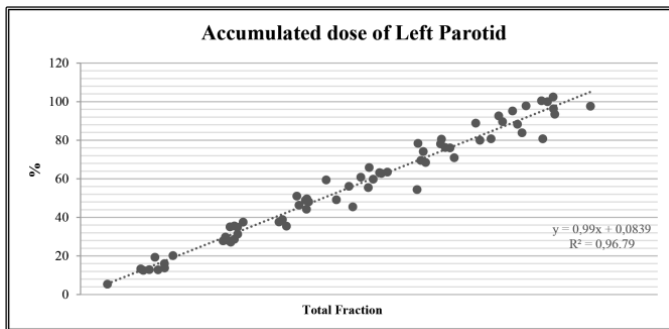


Figure 4. % Ratio of accumulated dose to planned for left parotid glands from all patients.

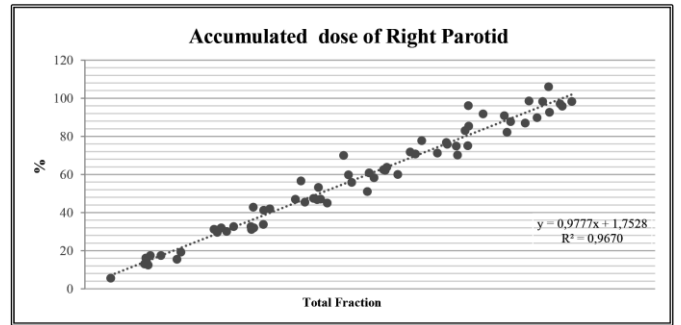


Figure 5. % Ratio of accumulated dose to planned for right parotid glands from all patients.

Table 4: Planned and accumulated dose for critical structures.

Patient ID	Medulla Spinalis		Left Parotid Gland		Right Parotid Gland	
	Planned	Accumulated	Planned	Accumulated	Planned	Accumulated
1	43.30	41.81	22.60	21.12	34.52	34.04
2	41.90	43.67	23.98	23.10	56.75	55.80
3	33.22	30.69	56.44	56.70	49.08	47.05
4	40.74	40.96	37.33	30.13	23.65	22.73
5	39.65	39.14	36.46	32.19	24.76	22.49
6	39.72	43.67	25.25	24.69	24.87	23.04
7	43.07	51.00	40.95	39.96	14.12	14.97
8	41.44	41.77	27.63	28.31	23.13	22.73
9	43.10	41.55	7.58	7.58	38.95	37.82
10	42.39	57.51	22.90	18.50	20.97	17.90
Mean	40.85	43.17	30.11	28.22	31.08	29.85

Table 5: Plan comparison for target volumes and organs at risk

	p Values	
PTV1 D _{mean}	0.083	> 0.05
PTV1 V ₁₀₀	0.216	> 0.05
PTV1 V ₉₅	0.041	< 0.05
PTV1 V ₉₀	0.093	> 0.05
PTV2 D _{mean}	0.250	> 0.05
PTV2 V ₁₀₀	0.072	> 0.05
PTV2 V ₉₅	0.060	> 0.05
PTV2 V ₉₀	0.142	> 0.05
PTV3 D _{mean}	0.188	> 0.05
PTV3 V ₁₀₀	0.010	< 0.05
PTV3 V ₉₅	0.004	< 0.05
PTV3 V ₉₀	0.060	> 0.05
Medulla Spinalis D _{mean}	0.211	> 0.05
Left Parotid Gland D _{mean}	0.045	< 0.05
Right Parotid Gland D _{mean}	0.070	> 0.05

*p = Significance

3.3. The Change in volume and COM displacement

Since head and neck cancer has a complex shape and many factors can affect tumor location and size, weight loss did not affect the volume shrinkage of targets by itself. The mean volume reduction in

PTV₁ was 3.3 % (range of 6.3%–1%), PTV₂ was approximately 7% (range of 18 – 0.8%), PTV₃ volume was 8.6% (range of 18 – 5.2%). The mean volume reduction in the right parotid gland was 11.7 % (range of 29.3 - 1.3 %). The mean volume reduction in the left parotid gland was 13.5 % (range of 25.9 - 5.7 %). The weekly volume change of the ROI was shown in Figure 6. The mean reduction in the distance between the parotid glands was 2.2 % (range of 3- 0.5 %). The average change in distance between the center of mass of the ROI and the parotid glands of ten patients during the treatment course was shown in Table 6. Even though the decrease in the distance was small, it caused a change in the dose delivered to the parotid glands.

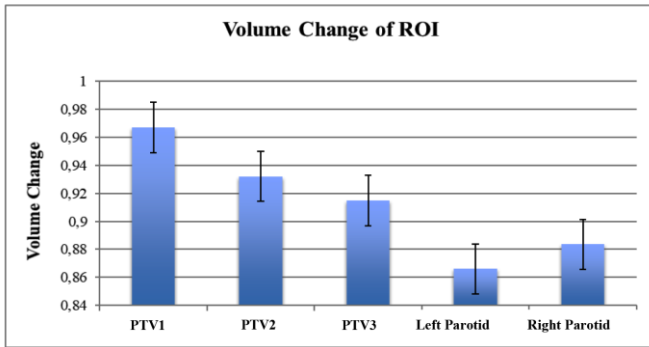


Figure 6. Volumetric Changes of ROI from 10 patients during the treatment course. The volumes were normalized to the planning volume. Average volume change was considered. Error bars are standard error.

Table 6. Average change in distance between center of mass of ROI and parotid glands of ten patients during the treatment course.

Patient ID	Average Change in Distance		
	Right Parotid - PTV1 (mm)	Left Parotid - PTV1 (mm)	Right Parotid - Left Parotid (mm)
1	6.41	6.27	11.12
2	7.56	5.15	10.58
3	6.72	6.93	12.64
4	4.74	9.06	12.55
5	4.36	8.29	11.70
6	8.01	5.97	11.89
7	5.18	7.31	20.01
8	5.37	7.46	12.04
9	8.46	4.41	11.19
10	7.45	6.75	12.00
Mean	6.42	6.76	12.57

Moreover, correlation analysis was applied to each patient to evaluate the effect of the change in volume and COM of critical structures and target volume on composite dose, was shown in Table 7. A strong negative correlation was obtained between volume change and composite dose of the left and right parotid glands ($r=-0.25$ and $r = -0.90$). The same analysis was also applied to determine the correlation between the COM displacement of the PTV - right parotid, PTV - left parotid, and both parotid glands. A strong positive correlation was obtained for the right parotid gland ($r=0.449$); however, this correlation was not statistically significant ($p=0.193$). Additionally, a strong positive correlation was also obtained for the left parotid ($r=0.826$) and this correlation was not statistically significant ($p=0.03$). Since the tumor location was closer to the left parotid gland and the shift was observed towards the left side, the COM displacement increased the composite dose of the left parotid gland.

Table 7. Correlation between the distance of parotid glands to PTV and accumulated dose.

	Correlation between Distance and Accumulated Dose	
	r values	p values
Right Parotid Gland	0.499 (> 0.05)	0.193 (> 0.05)
Left Parotid Gland	0.826 (> 0.05)	0.03 (< 0.05)

*r = Correlation Coefficient

*p = Significance

4. Discussion

Effective radiotherapy requires knowledge of the accumulated dose of ROI and the evaluation of the treatment results during the entire treatment course. Structural delineation and quantification of the change in volume of ROI between the planning CT and daily kVCT and/or MVCT images is possible with DIR (Weppeler, 2020). The obtained results based on in-room daily kVCT data showed that DIR is an essential tool for tracking the volume of the ROI and the distance between the target volume and critical structures because the image resolution of kV CT is superior to MVCT (Zhang, 2018). For this reason, many studies focused on the dose evaluation of OARs kV-kV alignment via DIR (Pukala, 2016; Branchini, 2017).

McIntosh et al. used an atlas-based approach to predict the dose. The predicted dose distribution was converted to a complete treatment plan via voxel-based dose-mimicking optimization. Target volume coverage and the dose of critical organs were evaluated. Based on their result, for target coverage, automated plans achieved of 0.6% overdose and 2.4% lower dose for OARs. Additionally, a GPU based-3D image framework was used to evaluate real-time dose accumulation and to track inter-fractional anatomical change for ROI. Moreover, the optical flow registration was used for the kV to kV alignment (McIntosh, 2017).

Elstrom et al. evaluated daily kV cone beam CT and deformable image registration for one patient. Fractional dose and change in volume of the parotid glands and PTVs were taken into account. The volume change between the planning and final fraction was 30% (Elström, 2010).

On the other hand, volume change and change in the center of mass for the parotid glands and target volumes were investigated in this study. Even though the DIR is an essential tool to track anatomical changes, there are still unknown questions regarding these changes that fluctuate among patients. In addition, weekly cumulative dose assessment plays a crucial role in quantifying whether the planned dose is delivered to the target while protecting organs at risk. DIR has been a vital method for radiation therapy applications; however, its integration into clinical practice requires further investigation. Moreover, dose accumulation via DIR is still under development and DIR cannot be used directly in clinical practice due to the limitations of dosimetric and clinical studies. On the other hand, DIR is a crucial step for adaptive radiation therapy ART; because modification of the treatment plan based on maintaining treatment objectives is aimed for ART.

5. Conclusion

One of the main problems in head and neck radiation therapy is the location of a tumor that is in close proximity to the surrounding structures. In addition, patients undergo many anatomical changes during the course of a radiation treatment. It was showed that, the in-house developed GPU based-3D image framework is an essential tool to allow for evaluation real time dose accumulation and tracking inter fractional volume change of ROI for adaptive radiation therapy. Additionally, the efficacy of radiation treatment depends on tracking geometric changes and their dosimetric consequences followed GPU-based algorithm systematically.

Acknowledgments

The authors are indebted to the University of California Los Angeles (UCLA) Radiation Oncology Department for their support providing head and neck cancer patients' data treated with tomotherapy. Theoretical calculations based on GPU-based deformable image registration algorithm and data analysis would have been impossible without the kind collaboration of Daniel Low, Professor, and Vice Chair of Medical Physics at UCLA, Sharon Qui, Anand Santhanam, and John Neylon.

Ethical Approval

For this type of study formal consent is not required in our Institution or The IRB was obtained without patient's information consent.

Informed Consent

Informed consent was obtained from all individual participants included in the study.

References

- 1) Atwell, D., Elks, J., Cahill, K., Hearn, N., Vignarajah, D., Lagopoulos, J., & Min, M. (2020). A review of modern radiation therapy dose escalation in locally advanced head and neck cancer. *Clinical Oncology*, 32(5), 330-341.
- 2) Toledano, I., Graff, P., Serre, A., Boisselier, P., Bensadoun, R. J., Ortholan, C., ... & Lapeyre, M. (2012). Intensity-modulated radiotherapy in head and neck cancer: results of the prospective study GORTEC 2004-03. *Radiotherapy and Oncology*, 103(1), 57-62.
- 3) O'Daniel, J. C., Garden, A. S., Schwartz, D. L., Wang, H., Ang, K. K., Ahamad, A., ... & Dong, L. (2007). Parotid gland dose in intensity-modulated radiotherapy for head and neck cancer: is what you plan what you get?. *International Journal of Radiation Oncology* Biology* Physics*, 69(4), 1290-1296.
- 4) Sharma, A., & Bahl, A. (2020). Intensity-modulated radiation therapy in head-and-neck carcinomas: Potential beyond sparing the parotid glands. *Journal of Cancer Research and Therapeutics*, 16(3), 425.
- 5) Heukelom, J., Kantor, M. E., Mohamed, A. S., Elhalawani, H., Kocak-Uzel, E., Lin, T., ... & Sonke, J. J. (2020). Differences between planned and delivered dose for head and neck cancer, and their consequences for normal tissue complication probability and treatment adaptation. *Radiotherapy and Oncology*, 142, 100-106.
- 6) Lowther, N. J., Marsh, S. H., & Louwe, R. J. (2020). Dose accumulation to assess the validity of treatment plans with reduced margins in radiotherapy of head and neck cancer. *Physics and imaging in radiation oncology*, 14, 53-60.
- 7) Kanehira, T., Svensson, S., van Kranen, S., & Sonke, J. J. (2020). Accurate estimation of daily delivered radiotherapy dose with an external treatment planning system. *Physics and Imaging in Radiation Oncology*, 14, 39-42.
- 8) Capelle, L., Mackenzie, M., Field, C., Parliament, M., Ghosh, S., & Scrimger, R. (2012). Adaptive radiotherapy using helical tomotherapy for head and neck cancer in definitive and postoperative settings: initial results. *Clinical Oncology*, 24(3), 208-215.
- 9) Loo, H., Fairfoul, J., Chakrabarti, A., Dean, J. C., Benson, R. J., Jefferies, S. J., & Burnet, N. G. (2011). Tumour shrinkage and contour change during radiotherapy increase the dose to organs at risk but not the target volumes for head and neck cancer patients treated on the Tomotherapy HiArt™ system. *Clinical oncology*, 23(1), 40-47.
- 10) Veiga, C., McClelland, J., Moinuddin, S., Lourenço, A., Ricketts, K., Annkah, J., ... & Royle, G. (2014). Toward adaptive radiotherapy for head and neck patients: feasibility study on using CT-to-CBCT deformable registration for “dose of the day” calculations. *Medical physics*, 41(3), 031703.
- 11) Fung, N. T. C., Hung, W. M., Sze, C. K., Lee, M. C. H., & Ng, W. T. (2020). Automatic segmentation for adaptive planning in nasopharyngeal carcinoma IMRT: time, geometrical, and dosimetric analysis. *Medical Dosimetry*, 45(1), 60-65.
- 12) Zhang, L., Wang, Z., Shi, C., Long, T., & Xu, X. G. (2018). The impact of robustness of deformable image registration on contour propagation and dose accumulation for head and neck adaptive radiotherapy. *Journal of Applied Clinical Medical Physics*, 19(4), 185-194.
- 13) Scaggion, A., Fiandra, C., Loi, G., Vecchi, C., & Fusella, M. (2020). Free-to-use DIR solutions in radiotherapy: Benchmark against commercial platforms through a contour-propagation study. *Physica Medica*, 74, 110-117.
- 14) Nobnop, W., Chitapanarux, I., Wanwilairat, S., Tharavichitkul, E., Lorvidhaya, V., & Sripan, P. (2019). Effect of deformation methods on the accuracy of deformable image registration from kilovoltage CT to tomotherapy megavoltage CT. *Technology in Cancer Research & Treatment*, 18, 1533033818821186.
- 15) Guerrero, T., Sanders, K., Castillo, E., Zhang, Y., Bidaut, L., Pan, T., & Komaki, R. (2006). Dynamic ventilation imaging from four-dimensional computed tomography. *Physics in Medicine & Biology*, 51(4), 777.
- 16) Weppeler, S., Schinkel, C., Kirkby, C., & Smith, W. (2020). Lasso logistic regression to derive workflow-specific algorithm performance requirements as demonstrated for head and neck cancer deformable image registration in adaptive radiation therapy. *Physics in Medicine & Biology*, 65(19), 195013.
- 17) Zhang, L., Wang, Z., Shi, C., Long, T., & Xu, X. G. (2018). The impact of robustness of deformable image registration on contour propagation and dose accumulation for head and neck adaptive radiotherapy. *Journal of Applied Clinical Medical Physics*, 19(4), 185-194.
- 18) Pukala, J., Johnson, P. B., Shah, A. P., Langen, K. M., Bova, F. J., Staton, R. J., ... & Meeks, S. L. (2016). Benchmarking of five commercial deformable image registration algorithms for head and neck patients. *Journal of applied clinical medical physics*, 17(3), 25-40.
- 19) Branchini, M., Fiorino, C., Dell'Oca, I., Belli, M. L., Perna, L., Di Muzio, N., ... & Broggi, S. (2017). Validation of a method for “dose of the day” calculation in head-neck tomotherapy by using planning ct-to-MVCT deformable image registration. *Physica Medica*, 39, 73-79.
- 20) McIntosh, C., Welch, M., McNiven, A., Jaffray, D. A., & Purdie, T. G. (2017). Fully automated treatment planning for head and neck radiotherapy using a voxel-based dose prediction and dose mimicking method. *Physics in Medicine & Biology*, 62(15), 5926.
- 21) Elström, U. V., Wysocka, B. A., Muren, L. P., Petersen, J. B., & Grau, C. (2010). Daily kV cone-beam CT and deformable image registration as a method for studying dosimetric consequences of anatomic changes in adaptive IMRT of head and neck cancer. *Acta oncologica*, 49(7), 1101-1108.